

SIMULATIONS OF VERTICALLY-COUPLED MICRODISK-RESONATORS BY 3-D VECTORIAL COUPLED MODE THEORY

Remco Stoffer¹, Kirankumar R. Hiremath², Manfred Hammer², Ladislav Prkna³, Jiří Čtyroký⁴

¹ PhoeniX BV, Enschede, The Netherlands
remco.stoffer@phoenixbv.com

² MESA⁺ Institute for Nanotechnology, University of Twente, Enschede, The Netherlands
k.r.hiremath@math.utwente.nl, m.hammer@math.utwente.nl

³ Laboratoire de Photonique et de Nanostructures, Centre National de la Recherche Scientifique, Marcoussis, France
Ladislav.Prkna@lpn.cnrs.fr

⁴ Institute of Radio Engineering and Electronics, Czech Academy of Sciences, Prague, Czech Republic
ctyroký@ure.cas.cz

SUMMARY

Fully vectorial 3D frequency-domain simulations of vertically coupled integrated-optical microdisk-resonators are described. The “rigorous” coupled mode theory model combines numerically computed bend modes of the cavity disk and guided modes of the straight bus waveguides.

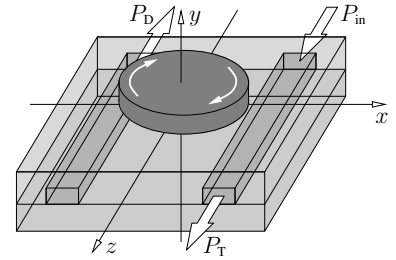
KEYWORDS

integrated optics, numerical modeling, coupled mode theory, cylindrical microdisk-resonators, vertical coupling

1 INTRODUCTION

Optical microresonators are at present discussed as building blocks for large-scale integrated optics [1, 2], where their range of applications includes in particular filter functions in optical wavelength-division multiplexing. Ref. [3] provides a recent overview of the field. As a typical example, for this contribution we focus on vertically coupled [4] microdisk-resonators, shown schematically in Figure 1.

Figure 1: Microdisk resonator, a 3-D configuration with a circular cavity on top of the two parallel bus waveguides. Two output ports through and drop each receive wavelength-dependent fractions P_T and P_D of the input power P_{in} .



The practical design relies crucially on an accurate knowledge of the strength of the interaction between the optical waves in the cavity and the bus waveguides, as a function of all geometrical and material parameters. While for horizontally coupled configurations effective-index-like reductions to 2-D problems can be attempted [5, 6, 7], the structure of Figure 1 requires simulations in three spatial dimensions. Also the vectorial properties of the optical fields may become relevant. Since rigorous 3-D numerical schemes must be considered almost prohibitively expensive, we investigate a coupled mode theory (CMT) model as a direct realization of the physical notions underlying the resonator design.

Manifold CMT variants for different domains of applications have been proposed [8, 9, 10, 11]. Among these several studies (see e.g. [12, 5, 6, 7]) deal with the evanescent interaction of waves in circularly bent and straight waveguides, where most of these describe 2-D implementations. Apparently so far only a few, rather heuristic 3-D studies [13, 14] exist. This contribution refers to a fully vectorial 3-D CMT implementation, applicable in principle to an arbitrary number of possibly multi-modal straight or circularly bent waveguides. The formulation is based on a variational or reciprocity technique [9, 15]; it highly resembles the previous 2-D version in Refs. [16, 17].

The CMT approach requires basis solutions for the constituting elementary problems. These are mode profiles of straight waveguides and disk profiles with 2-D cross sections, the computation of which is in itself nontrivial. Here we could profit from a solver based on film-mode matching, as described in Refs. [18, 19, 20]. The analytical field representation on a laterally or radially unbounded cross section proves to be highly advantageous for the evaluation of the CMT integrals.

2 MODELING BACKGROUND

In line with the most common ringresonator model [21, 11, 22], we assume that the interaction between optical waves in the bus waveguides and the cavity can be restricted to two “coupler regions” where the cores are in closest proximity. Figure 2 shows a top view and cross section of the interaction region, and the enclosure by a rectangular computational window. What follows is meant for the frequency domain; all optical waves oscillate in time $\sim \exp(i\omega t)$ with real frequency $\omega = 2\pi/(\lambda\sqrt{\epsilon_0\mu_0})$, given by the vacuum wavelength λ .

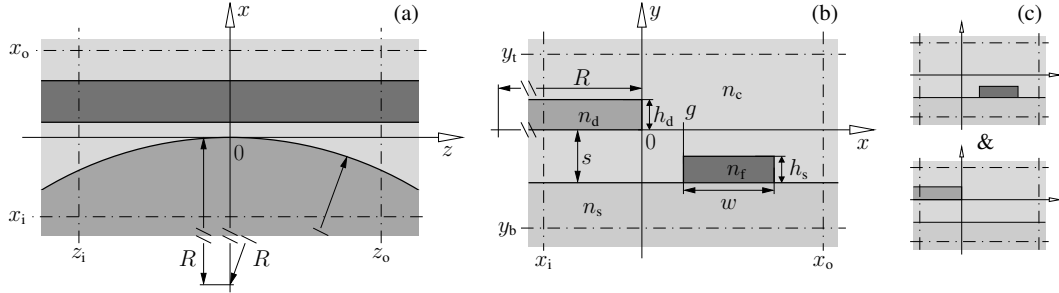


Figure 2: (a): Top view of the coupler region, for a cavity disk with radius R . (b): Cross section through the symmetry plane $z = 0$. The relative core positions are defined by the vertical distance s and the position (“gap”) g of the left flank of the straight core (negative g indicates overlapping components). (c): The total optical field is assumed to be well represented by modal solutions of the straight waveguide (top) and the cavity (bottom). Geometrical and material parameters: $w = 2.0 \mu\text{m}$, $h_s = 140 \text{ nm}$, $n_f = 1.98$, $n_s = 1.45$, $n_c = 1.4017$, $n_d = 1.6062$, $h_d = 1.0 \mu\text{m}$, $R = 100 \mu\text{m}$. Numerical parameters for the CMT integration: $\Delta x = 40 \text{ nm}$, $\Delta y = 20 \text{ nm}$, $\Delta z = 2.0 \mu\text{m}$ (see text), computational window $[x_i, x_o] = [-12, 4] \mu\text{m}$, $[y_b, y_t] = [-4 \mu\text{m} - s, 4 \mu\text{m} - s]$, $[z_i, z_o] = [-30, 30] \mu\text{m}$.

The coupled mode theory model rests on the assumption that the optical electromagnetic field \mathbf{E} , \mathbf{H} for the composite coupler structure with permittivity ϵ can be adequately represented as a superposition of a number of known fields \mathbf{E}_m , \mathbf{H}_m for problems with permittivity ϵ_m . For the coupler of Figure 2, the sketches (c) indicate a natural division. We choose the Cartesian z -coordinate as the evolution variable for all basis fields, such that the CMT ansatz reads:

$$\mathbf{E}(x, y, z) = \sum_m A_m(z) \mathbf{E}_m(x, y, z), \quad \mathbf{H}(x, y, z) = \sum_m A_m(z) \mathbf{H}_m(x, y, z). \quad (1)$$

$\mathbf{E}_m(x, y, z)$ and $\mathbf{H}_m(x, y, z)$ consist of power normalized [23] mode profiles, multiplied by the exponential dependences on the respective propagation coordinate, all transformed to Cartesian coordinates.

Lorentz’ reciprocity theorem [9] allows to derive evolution equations for the amplitudes A_m . Application to the ansatz (1) leads, after further manipulations [16], but without additional heuristics or approximations, to the coupled mode equations

$$\sum_m d_z A_m \int (\mathbf{E}_m \times \mathbf{H}_k^* + \mathbf{E}_k^* \times \mathbf{H}_m) \cdot \mathbf{z} \, dx \, dy = -i\omega\epsilon_0 \sum_m A_m \int (\epsilon - \epsilon_m) \mathbf{E}_m \cdot \mathbf{E}_k^* \, dx \, dy. \quad (2)$$

After numerically solving this system of equations for the amplitudes A_m , by projecting the solution onto the straight waveguide modes (“taking overlap integrals”, an essential step [16]), one obtains the scattering matrix \mathbf{S} for the coupler region. The element S_{oi} (“coupling coefficient”) corresponds to the interaction between input mode i and output mode o , where (power normalized basis modes) $|S_{oi}|^2$ can be interpreted as the relative power transferred to mode o , given a unit input in mode i . Once these matrices and the propagation constants of the cavity modes are at hand, evaluation of the power transfer of the full microresonator device is straightforward [11, 22]. Scans over the wavelength parameter allow to determine the spectral response.

The CMT basis fields are generated by a rigorous, fully vectorial (bend) mode solver based on the film-mode-matching (FMM) method. The semianalytical procedure relies on a division of the cross section plane into slices with laterally / radially constant permittivity. Per slice the field is expanded into modes of 1-D multilayer slab waveguides. 3-D modes are found where the expansions can be connected such that continuity and external boundary conditions are satisfied. Cf. Refs. [18, 19, 20] for algorithmic details. Only few numerical parameters enter: the numbers of slab modes M_s per slice and polarization direction, and the vertical computational window $[y_b^M, y_t^M]$. Further the CMT model requires numerical procedures for the repeated quadrature of the x - y -integrals in Eq. (2) (so far a trapezoidal rule) and for the integration of the system (2) of ordinary differential equations (a fourth order Runge-Kutta scheme). The extensions of the computational window and the integration stepsizes Δx , Δy , and Δz enter as numerical parameters.

Due to the lack of 3-D reference data, we had to rely on indirect means for a validation of the implementation: Similar 2-D procedures can be verified directly [16, 17]. For the case of parallel straight waveguides, numerically exact 3-D reference results can be generated by standard “supermode” analysis. CMT values for the S_{ss} coefficients in bend-straight coupler configurations have been compared with semivectorial beam-propagation simulations [24]. Finally, we observed that the power balance and reciprocity constraints are satisfied with reasonable accuracy.

3 COUPLER SIMULATIONS

The present disk structure supports multiple modes with small attenuation; the three lowest order vectorial, TE-like fields are taken into account in the following simulations. Table 1 lists the (complex) effective indices of the disk modes for vertical separations s of 0.5 and 1.0 μm . These are meant relative to the rim of the disk, i.e. the modal fields evolve

with the angular coordinate θ in the cylindrical disk coordinate system as $\sim \exp(kn_{\text{eff}}R\theta)$, where R is the disk radius as introduced in Figure 2. Figure 3 illustrates the mode profiles for the smaller separation $s = 0.5 \mu\text{m}$.

	$s = 0.5 \mu\text{m}$	$s = 1.0 \mu\text{m}$
TE ₀	$1.503778 - i 1.35 \cdot 10^{-9}$	$1.503450 - i 1.53 \cdot 10^{-9}$
TE ₁	$1.474931 - i 1.77 \cdot 10^{-6}$	$1.474585 - i 4.96 \cdot 10^{-7}$
TE ₂	$1.451487 - i 5.05 \cdot 10^{-5}$	$1.451093 - i 1.56 \cdot 10^{-5}$

Table 1: Effective indices n_{eff} of the disk modes of Figure 3 related to the disk rim. The bus core guides one TE-like mode with an effective mode index of 1.48229.

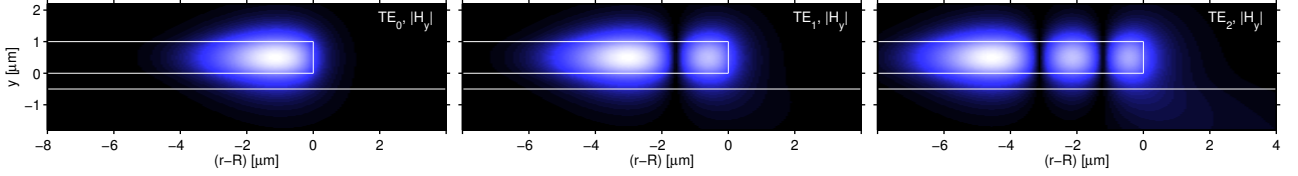


Figure 3: The three lowest order TE-like bend mode profiles supported by the disk for $s = 0.5 \mu\text{m}$; absolute values $|H_y|$ of the dominant magnetic component. For the vertical symmetry plane of the coupler, the radial coordinate r (with offset R) coincides with the x -coordinate in Figure 2. Mode analysis parameters: $M_s = 200$, $[y_b^M, y_t^M] = [-10 \mu\text{m} - s, 7 \mu\text{m} - s]$.

With four basis modes the CMT simulations generate 4×4 scattering matrices. Figure 4 summarizes the dependence of the 16 coefficients S_{oi} on the “gap” position, for $s = 1.0 \mu\text{m}$. $g = 0$ indicates a setting where, in a top view as in Figure 2(a), the inner flank of the bus waveguide just touches the rim of the cavity disk. Subscripts s, b0, b1, and b2 identify the modes of the straight waveguide and the three bend modes of the cavity, respectively.

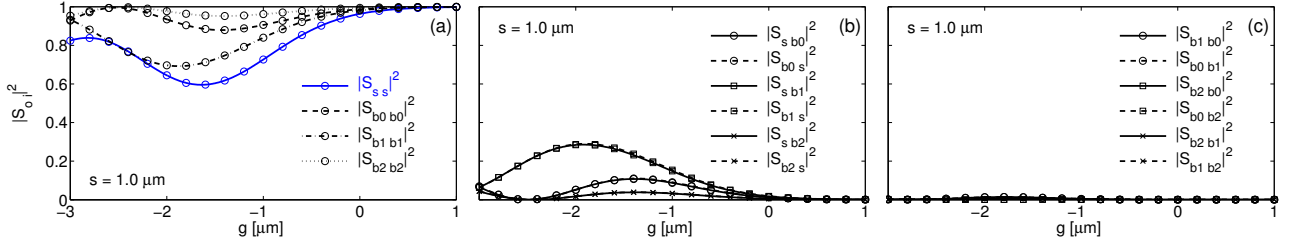


Figure 4: Scattering matrix coefficients $|S_{oi}|^2$ for $s = 1.0 \mu\text{m}$ versus the lateral disk position g . (a): the self-coupling power of each mode, (b) the cross-coupling power coefficients between the mode of the straight waveguide and the bend fields, (c): the cross-coupling coefficients for the bend modes.

Beyond power conservation, the excellent agreement of the dashed and continuous lines in Figure 4(b, c) indicates that our CMT implementation satisfies the reciprocity properties [9, 22, 23] of the symmetric coupler structure remarkably well. For each pair of modes m and n , one finds the power $|S_{nm}|^2$ transferred from mode m at $z = -z_0$ to mode n at $z = z_0$ to be equal to the power transfer $|S_{mn}|^2$ from mode n at $z = -z_0$ to mode m at $z = z_0$.

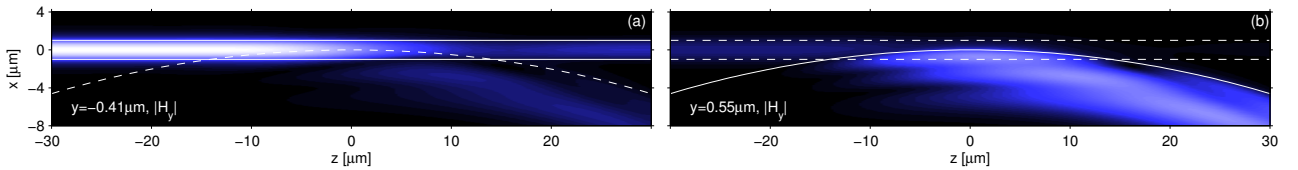


Figure 5: Coupled mode propagation along the coupler region of Figure 2, for $s = 0.5 \mu\text{m}$ and $g = -1.0 \mu\text{m}$; absolute values $|H_y|$ of the dominant magnetic component. At $z_i = -30 \mu\text{m}$ the guided TE-like mode of the straight waveguide is launched. Horizontal field cross sections at $y = -0.41 \mu\text{m}$, close to the center of the straight core (a) and at $y = 0.55 \mu\text{m}$, near the center of the disk (b).

Given the numerical solution of Eq. (2) and the mode profile data, the CMT model provides full information about the electromagnetic field in the coupler region. Figure 5 illustrates the field evolution after excitation in the straight waveguide, for a configuration $s = 0.5 \mu\text{m}$, $g = -1.0 \mu\text{m}$ with strong interaction. One observes the depleting of the straight waveguide mode at the level of the bus core (a) and the beginning of the beating of the three cavity modes at a higher position inside the disk (b).

4 RESONATOR SPECTRA

Figure 6 shows examples for resonator spectra of symmetric devices for different relative positions of bus waveguides and cavity, evaluated on the basis of the former coupler scattering matrices. For the large separation (a) one finds a periodically repeated array of three well separated, narrow peaks in the dropped power or dips in the transmitted power,

respectively. By inspecting the relative amplitudes of the disk modes at resonance, one can assign the first, broadest and least pronounced dip to the second order, most lossy disk mode b2. The second peak with almost 100% dropped power can be ascribed to the fundamental mode b0, while the last resonance is due to the first order field b1. As expected, for the smaller separation (b) with stronger interaction the quality of the resonances decreases. The peaks are shifted moderately, they broaden, become more pronounced, and start to overlap.

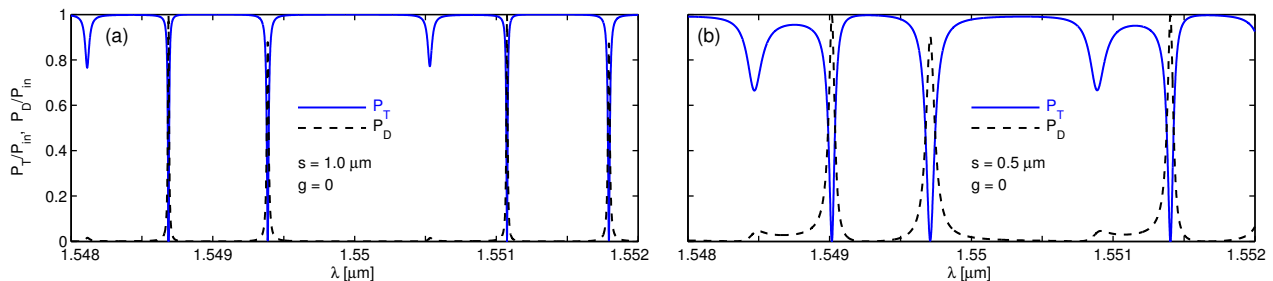


Figure 6: Relative dropped and transmitted power levels P_D , P_T versus the vacuum wavelength λ , for symmetrical microresonators with couplers according to Figure 2, for horizontal cavity position $g = 0$ and vertical separations $s = 1.0 \mu\text{m}$ (a) and $s = 0.5 \mu\text{m}$ (b).

5 CONCLUSIONS

Based on numerically computed mode profiles of straight bus waveguides and the circular cavity, a 3-D, fully vectorial frequency-domain coupled mode theory model for the interaction between cavity and bus waveguides has been established, that constitutes a robust, efficient, and reasonably accurate tool for ab-initio design of circular optical microresonators. In contrast to any “general purpose” rigorous numerical methods, the CMT approach yields directly well defined values for the physical quantities (coupler scattering matrix coefficients, cavity mode amplitudes) that constitute the standard description of optical microresonators, as an ideal basis for the practical design of resonator elements. Beyond the coupling coefficients, in principle the entire 3-D field for the coupling region, resonator spectra, and also the full, wavelength dependent optical field for the entire microresonator can be evaluated. The procedures have been exemplified by means of a multimode, vertically coupled microdisk-resonator, where the approach allows to easily access a wide range of geometrical design parameters.

ACKNOWLEDGMENTS

This work has been supported by the European Commission (project IST-2000-28018, ‘NAIS’ [2]). The authors thank E. van Groesen, H. J. W. M. Hoekstra, and the colleagues in the NAIS project for many fruitful discussions.

REFERENCES

- [1] B. E. Little, S. T. Chu, W. Pan, and Y. Kokubun. *IEEE Photonics Technology Letters.*, 12(3):323–325, 2000.
- [2] Next-generation active integrated optic subsystems, 2001-2004. Information society technologies programme of the European Commission, project IST-2000-28018, <http://www.mesap.us.utwente.nl/nais/>.
- [3] M. Bertolotti, A. Driessen, and F. Michelotti, editors. *Microresonators as building blocks for VLSI photonics*, volume 709 of AIP conference proceedings. American Institute of Physics, Melville, New York, 2004.
- [4] B. E. Little, S. T. Chu, W. Pan, D. Ripin, T. Kaneko, Y. Kokubun, and E. Ippen. *IEEE Photonics Technology Letters*, 11(2):215–217, 1999.
- [5] B. E. Little, S. T. Chu, H. A. Haus, J. Foresi, and J.-P. Laine. *Journal of Lightwave Technology*, 15(6):998–1005, 1997.
- [6] M. K. Chin and S. T. Ho. *Journal of Lightwave Technology*, 16(8):1433–1446, 1997.
- [7] D. J. W. Klunder et. al. *Applied Physics B*, 73:603–608, 2001.
- [8] D. G. Hall and B. J. Thompson, editors. *Selected Papers on Coupled-Mode Theory in Guided-Wave Optics*, volume MS 84 of SPIE Milestone Series. SPIE Optical Engineering Press, Bellingham, Washington USA, 1993.
- [9] C. Vassallo. *Optical Waveguide Concepts*. Elsevier, Amsterdam, 1991.
- [10] D. Marcuse. *Theory of Dielectrical Optical Waveguides, 2nd edition*. Academic Press, London, 1991.
- [11] K. Okamoto. *Fundamentals of Optical Waveguides*. Academic Press, San Diego, 2000.
- [12] D. R. Rowland and J. D. Love. *IEE Proc., Pt. J*, 140(3):177–188, 1993.
- [13] J. A. Loaiza et. al. IEEE/LEOS Benelux Chapter, Proc. 5th Annual Symposium, Delft, 215–218, 2000.
- [14] A. Stumpf, J. Kunde, U. Gubler, A.-C. Pliska-Leduff, and C. Bosshard. *Optical and Quantum Electronics*, 35:1205–1213, 2003.
- [15] M. Lohmeyer, N. Bahlmann, O. Zhuromsky, and P. Hertel. *Optical and Quantum Electronics*, 31:877–891, 1999.
- [16] R. Stoffer, K. R. Hiremath, and M. Hammer. Comparison of coupled mode theory and FDTD simulations of coupling between bent and straight optical waveguides. volume 709 of AIP conference proceedings [3], pages 366–377, 2004.
- [17] K. R. Hiremath, R. Stoffer, and M. Hammer. IEEE/LEOS Benelux Chapter, Proc. 9th Annual Symposium, Ghent, Belgium, 79–82, 2004.
- [18] L. Prkna. *Rotationally symmetric resonant devices in integrated optics*. Faculty of Mathematics and Physics, Charles University, Prague, and Institute of Radio Engineering and Electronics, Academy of Sciences of the Czech Republic, Prague, Czech Republic, 2004. Ph.D. Thesis.
- [19] L. Prkna, M. Hubálek, and J. Čtyrůk. *IEEE Photonics Technology Letters*, 16(9):2057–2059, 2004.
- [20] L. Prkna, M. Hubálek, and J. Čtyrůk. Field Modelling of Circular Microresonators by Film Mode Matching. *IEEE Journal of Selected Topics in Quantum Electronics*, 2004. (accepted).
- [21] E. A. J. Marcanti. *The Bell System Technical Journal*, September:2103–2132, 1969.
- [22] M. Hammer, K. R. Hiremath, and R. Stoffer. Analytical approaches to the description of optical microresonator devices. volume 709 of AIP conference proceedings [3], pages 48–71, 2004.
- [23] K. R. Hiremath, M. Hammer, R. Stoffer, L. Prkna, and J. Čtyrůk. Analytical approach to dielectric optical bent slab waveguides. *Optical and Quantum Electronics*, 2005. (accepted).
- [24] OlympIOs Integrated Optics Software. C2V, P.O. Box 318, 7500 AH Enschede, The Netherlands; <http://www.c2v.nl/software/>.